# AUTOMATIC GEOGRAPHIC OBJECT BASED MAPPING OF STREAMBED AND RIPARIAN ZONE EXTENT FROM LIDAR DATA IN A TEMPERATE RURAL URBAN ENVIRONMENT, AUSTRALIA

K. Johansen [a,b] *, D. Tiede [c], T. Blaschke [c], S. Phinn [a,b], L. A. Arroyo [a,b, d]

[a] Joint Remote Sensing Research Program
[b] Centre for Spatial Environmental Research, School of Geography, Planning and Environmental Management, The University of Queensland, Brisbane, QLD 4072, Australia - (k.johansen, s.phinn)@uq.edu.au
[c] Z_GIS Centre for Geoinformatics, Salzburg University, Schillerstrasse 30, 5020 Salzburg, Austria – (dirk.tiede, Thomas.Blaschke)@sbg.ac.at
[d] Centro de Investigacion del Fuego, Fundacion General del Medio Ambiente de Castilla La Mancha, 45071 Toledo, Spain - Lara.Arroyo@uclm.es

**Commission VI, WG IV/4**

**KEY WORDS:** Geographic object based image analysis, LiDAR, Streambed, Riparian zone, Australia, pixel-based object resizing

**ABSTRACT:**

This research presents a time-effective approach for mapping streambed and riparian zone extent from high spatial resolution LiDAR derived products, i.e. digital terrain model, terrain slope and plant projective cover. Geographic object based image analysis (GEOBIA) has proven useful for feature extraction from high spatial resolution image data because of the capacity to reduce effects of reflectance variations of pixels making up individual objects and to include contextual and shape information. This functionality increases the likelihood of generalizing classification rules, which may lead to the development of automated mapping approaches. The LiDAR data were captured in May 2005 with 1.6 m point spacing and included first and last returns and an intensity layer. The returns were classified as ground and non-ground points by the data provider. The data covered parts of the Werribee Catchment in Victoria, Australia, which is characterized by urban, agricultural, and forested land cover types. Field data of streamside vegetation structure and physical form properties were obtained in April 2008. The field data were used both for calibration of the mapping routines and to validate the mapping results. To improve the transferability of the rule set, the GEOBIA approach was developed for an area representing different riparian zone environments, i.e. urbanised areas, agricultural areas, and hilly forested areas. Results show that mapping streambed extent ($R^2$ = 0.93, RMSE = 3.3 m, n = 35) and riparian zone extent ($R^2$ = 0.74, RMSE = 3.9, n = 35) from LiDAR derived products can be automated using GEOBIA. This work lays the foundation for automatic feature extraction of biophysical properties of riparian zones to enable derivation of spatial information in an accurate and time-effective manner suited for natural resource management agencies.

## 1. INTRODUCTION

### 1.1 Riparian Zones

Riparian zones along rivers and creeks have long been identified as important elements of the landscape due to the flow of species, energy, and nutrients, and their provision of corridors providing an interface between terrestrial and aquatic ecosystems (Apan et al., 2002; Naiman and Decamps, 1997). Threats to riparian zones are compounded by increased anthropogenic development and disturbances in or adjacent to these environments. Riparian zones and related vegetation form corridors with distinct environmental functions and processes. To assess these functions and processes environmental indicators of riparian vegetation structure and physical form of stream banks are normally used (Werren and Arthington, 2002). Two of the most important environmental indicators to assess are the streambed extent and the riparian zone extent. Mapping streambed extent allows determination and assessment of a number of riparian environmental

indicators such as streambed width, vegetation overhanging the stream, identification of stream banks for stream bank condition assessment, and water body assessment. Mapping the extent of the riparian zones defines the area within which riparian environmental indicators such as riparian zone width, plant projective cover (PPC), vegetation continuity, and other vegetation structural parameters are to be assessed. Hence, a starting point and requirement for riparian zone assessment is the accurate mapping and identification of streambed and riparian zone extents.

### 1.2 Remote Sensing of Riparian Zones

Several papers have concluded that the use of remotely sensed image data are required for assessment of riparian zones for areas > 200 km of stream length, as field surveys become cost prohibitive at those spatial scales (Johansen et al., 2007). The availability of data from high spatial resolution sensors such as the IKONOS, QuickBird and Geoeye-1 satellite sensors and

---

* Corresponding author

airborne multi-spectral, hyper-spectral and light detection and ranging (LiDAR) sensors have opened up new opportunities for development of operational mapping and monitoring of small features such as narrow riparian zones (Hurtt et al., 2003). Johansen et al. (2010) found airborne LiDAR data to be suitable for mapping a number of riparian environmental indicators. They also assessed the use of LiDAR data for mapping streambed and riparian zone extents using geographic object based image analysis (GEOBIA) and obtained high mapping accuracies of streambed and riparian zone widths. However, the rule sets applied to automatically map streambed and riparian zone extents were found time-consuming, especially for large area mapping because of the use of near pixel-level segmentations and region growing algorithms. The rule sets were also found to work only in areas with streambeds clearly defined by bordering steep bank slopes. The objective of this work was to develop a new, time-effective and transferable approach for mapping streambed and riparian zone extents from high spatial resolution LiDAR derived products, i.e. digital terrain model (DTM), terrain slope and PPC.

## 2. DATA AND METHODS

### 2.1 Study Area

The riparian study area was located along the Werribee and Lerderderg Rivers and Pyrites, Djerriwarrh, and Parwan Creeks in the urbanized and cultivated temperate Werribee Catchment in Victoria, 50 km northwest of Melbourne (Figure 1). The Werribee River is the major drainage stream emanating from the Werribee Catchment, and the rivers and creeks nominated for the study area confluence with it. In the northern part of the study area remnant forests of the Central Victorian Upland bioregion exist. The northern terrain is characterized by small streams cutting courses and gorges in heavily eroded hills. The water flow of the streams is generally south from the hilly areas until reaching the confluence with the Werribee River, where flows turns east and then southeast before eventually draining into Port Phillip Bay. The southern half of the study area is part of the flat Victorian Volcanic Plain bioregion characterized by disturbed terrain with agricultural (grazing and cultivation) and urban land use features.
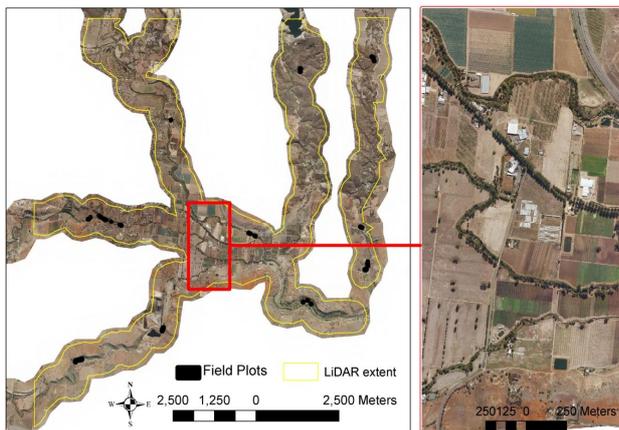


Figure 1. Area covered by the LiDAR data in the Werribee Catchment and zoomed in section showing more details of the Lerderderg River (north), Werribee River (middle), and Parwin Creek (south). Thirty-five field plots were assessed. UltracamD image data are used to illustrate the LiDAR data coverage.

### 2.2 Field Data Acquisition

A field campaign was carried out in the Werribee Catchment between 31 March and 4 April 2008. The field data acquisition was designed to match the spatial resolution of the LiDAR data. Field measurements were obtained along transects located perpendicular to the streams of several biophysical vegetation structural and physical form parameters. However, the only field measurements used in this research included: (1) streambed width; (2) riparian zone width; (3) PPC; and (4) stream bank slope and elevation. Streambed width was measured with a laser range finder. Riparian zone width was measured with a tape measure from the toe of the stream bank to the external perimeter defined by the stream bank flattening and the vegetation species that no longer dependant on the stream for survival. Existing high spatial resolution optical image data were used to locate in-situ ground control points visible in both the field and image data to complement GPS points to precisely overlay field and image data. GPS measurements were obtained by averaging the position of the start and end of each transect until the estimated positional error was below 2.0 m.

### 2.3 LiDAR Data Acquisition and Preparation

The LiDAR data used in this study were captured using the Optech ALTM3025 sensor between 7 and 9 May 2005 for the study area. The LiDAR data were captured with an average point spacing of 1.6 m (0.625 points per $m^2$) and consisted of two returns, first and last returns, as well as intensity. The LiDAR returns were classified as ground or non-ground by the data provider using proprietary software. The flying height when capturing the LiDAR data was approximately 1500 m above ground level. The maximum scan angle was set to 40º with a 25% overlap of different flight lines. The estimated vertical and horizontal accuracies were < 0.20 m and < 0.75 m respectively. GPS base stations were used for support to improve the geometric accuracy of the dataset. The LiDAR data were deemed suitable for integration with the field data despite the time gap between the data acquisitions. This assumption was based on existing riparian field data from 2004 provided by the Victorian Depart of Sustainability and Environment and rainfall data confirming lower than average rainfalls between 2005 and 2008 and hence no likely changes in streambed and riparian zone extents within the study area.

The following three LiDAR products were produced for use in the GEOBIA: DTM; terrain slope; and fractional cover count converted to PPC (Figure 2). The DTM was produced at a pixel size of 1 m using an inverse distance weighted interpolation of returns classified as ground hits. From this DTM, the rate of change in horizontal and vertical directions was calculated to produce a terrain slope layer. Fractional cover count defined as one minus the gap fraction probability, was calculated from the proportion of counts from first returns 2 m above ground level within 5 m x 5 m pixels. The height threshold of 2 m above ground was also used in the field for measuring PPC. A detailed explanation of calculating PPC from fractional cover counts can be found in Armston et al. (2009). These LiDAR derived raster products were used for GEOBIA to map the streambed and riparian zone extents. A shapefile representing the location of the stream centres within the study area was provided by the Victorian Department of Sustainability and Environment and used in the GEOBIA.
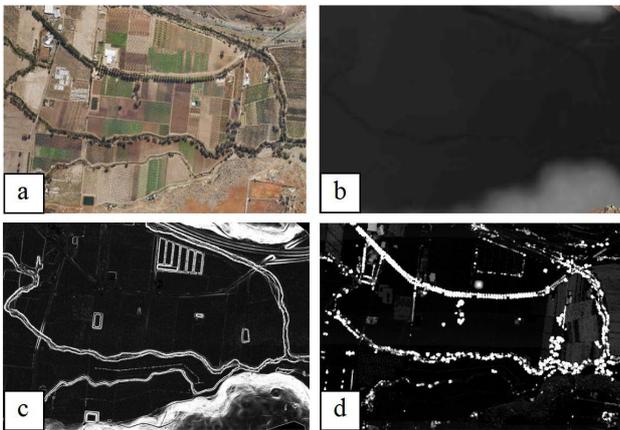
Figure 2. Optical image (a) showing part of the study area and corresponding LiDAR derived raster products, including: (b) DTM; (c) slope; and (d) PPC. Bright areas indicate high values and dark areas indicate low values.

## 2.4 Classifying Streambeds

The streambed extent was defined as the continuous flat low-lying area between the toe of one bank to the toe of the opposite bank, which is generally where water is flowing. Mapping the extent of streambeds cannot be done simply by setting an elevation threshold from a DTM, as upstream areas will have different elevations to downstream areas. Hence, an approach was developed using the DTM and terrain slope layers (Johansen et al., 2010). eCognition 8 was used for the development of a rule set for time-efficient mapping of the streambed extent using the DTM, slope and rasterised polyline representing the approximate stream centreline.

Pixel-based object resizing algorithms are new algorithms introduced in eCognition 8, which allow the growing, shrinking and coating of objects by directly connecting to single pixels of the underlying data sets. The growing mode adds and merges one row of pixels on the outside of an existing object. Through multiple loops, multiple layers of pixels can be added. The shrinking mode subtracts one row of pixels from an original object through classification of this row of objects as a separate class. The coating mode cuts one row of pixels around an existing object and classifies it to a separate class, similar to buffering (Figure 3) (eCognition, 2010). Conditions can be set for adding, subtracting and cutting layers of pixels, e.g. only pixels below a set threshold may be considered. Through looping, multiple layers of pixels can be added, subtracted or cut. These algorithms may replace some computational intensive object growing algorithms, which rely heavily on topological calculations.

Initially, a multi-threshold segmentation was used to classify the stream centreline (Figure 4a). The next stage used the pixel-based object resizing algorithm to grow the stream centreline through two loops as long as the slope did not exceed 12º and the unclassified candidate pixels, i.e. pixels surrounding the stream centreline, were < 0.5 m in elevation compared to the stream centreline. This pragmatic approach was used to widen the stream centreline to 5 m through the two loops. Subsequently, the pixel-based object growing was used to grow the widened stream centreline as along as the unclassified candidate pixels surrounding the stream centreline were < 0.01 m in elevation compared to the widened stream

centreline using an empirically derived surface tension of > 0.2 within an 11 x 11 pixel window (Figure 4b). The pixel-based object resizing algorithm was then used to further grow the streambed as long as the slope did not exceed 12º and the unclassified candidate pixels were < 0.08 m in elevation compared to the stream centreline. A surface tension of > 0.5 within an 11 x 11 pixel window was used (Figure 4c). Finally, objects enclosed by the streambed were merged with the streambed objects (Figure 4d).
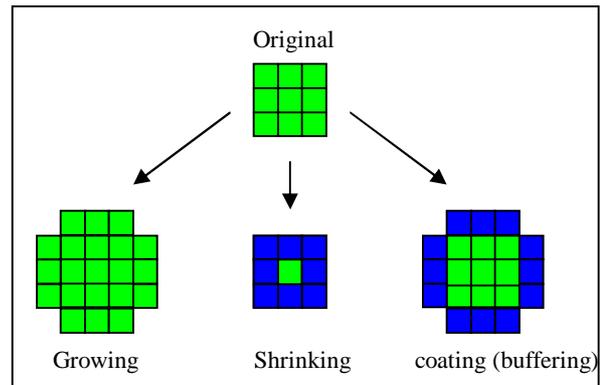


Figure 3. Pixel-based object resizing modes showing the principles of growing, shrinking and coating.

## 2.5 Classifying Riparian Zones

The classification of the streambeds and riparian zones was based on the approach developed by Johansen et al. (2010). However, as this approach used several chessboard segmentations and image object fusion, merging and region-growing algorithms, it was found very time-consuming for use over large areas. The approach presented here focused on more time-effective mapping of the riparian zones using new algorithms from eCognition 8. Riparian zone extent was defined as the area between the streambed and the external perimeter defined by a significant change and terrain slope (top of bank) and vegetation structure and species.

The classification of the streambed was used to identify the streamside edge of the riparian zone. A number of steps were used for mapping the riparian zones, again focusing on the use of the pixel-based object resizing algorithm. To include distance measures around the streambed, it was not sufficient only to use the pixel-based growing algorithms starting from the streambed, as non-connected elements were missing. Therefore, distance buffers were first created using the coating mode and then followed by the pixel-based object resizing algorithm using the shrinking mode. The shrinking algorithm was initially used to map PPC > 40% (Figure 5a). The shrinking algorithm was then used within the 25 m buffer to identify areas with > 10º slope, as these can be assumed to belong to the riparian zone even if not vegetated. Gaps enclosed by the streambed and with PPC > 40% and slope > 10º were also assumed to be part of the riparian zone (Figure 5b). Those riparian elements, including objects with > 40% PPC, > 10º slope and gaps were merged and those objects not in contact with the streambed were omitted. Elevation differences between the streambed and the external perimeter of the riparian zone provided very useful information for mapping riparian zone extent to ensure riparian zones do not extend into non-riparian areas in hilly landscapes.
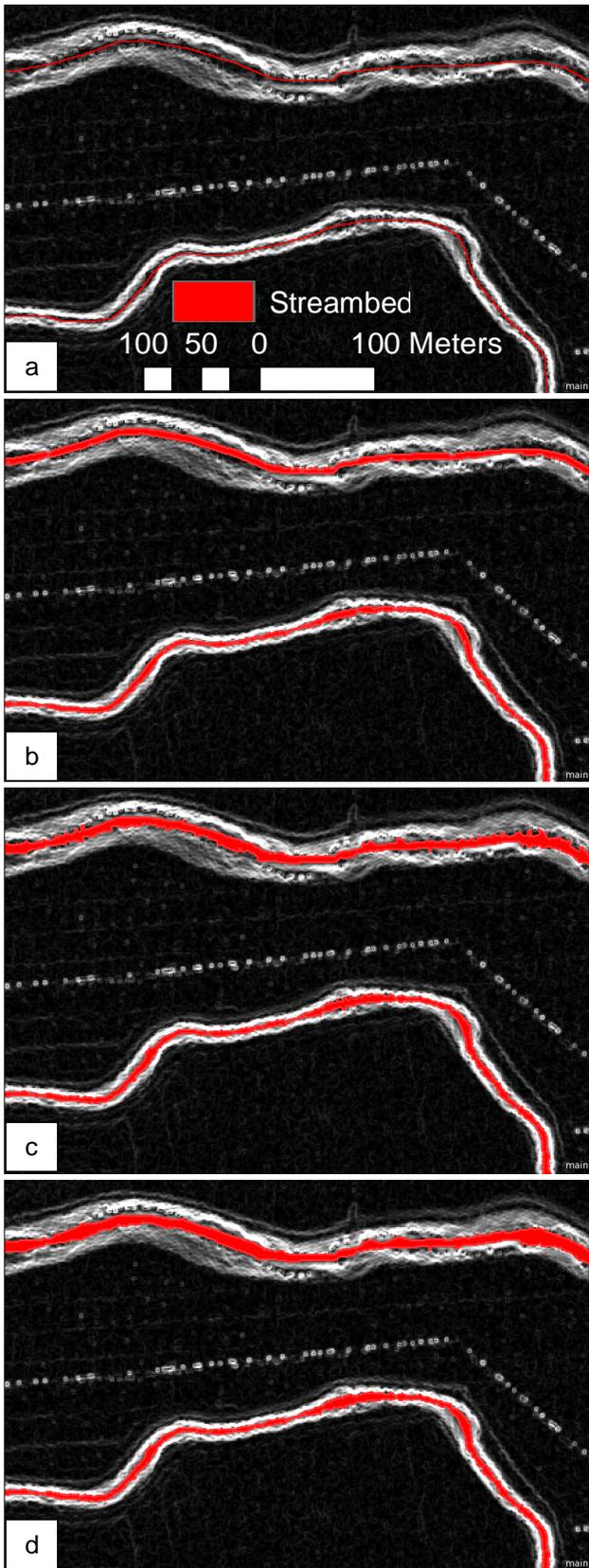
Figure 4. Mapping the streambed from the LiDAR derived DTM and slope layers and a rasterised polyline representing the stream centreline. The slope layer is used as a backdrop.
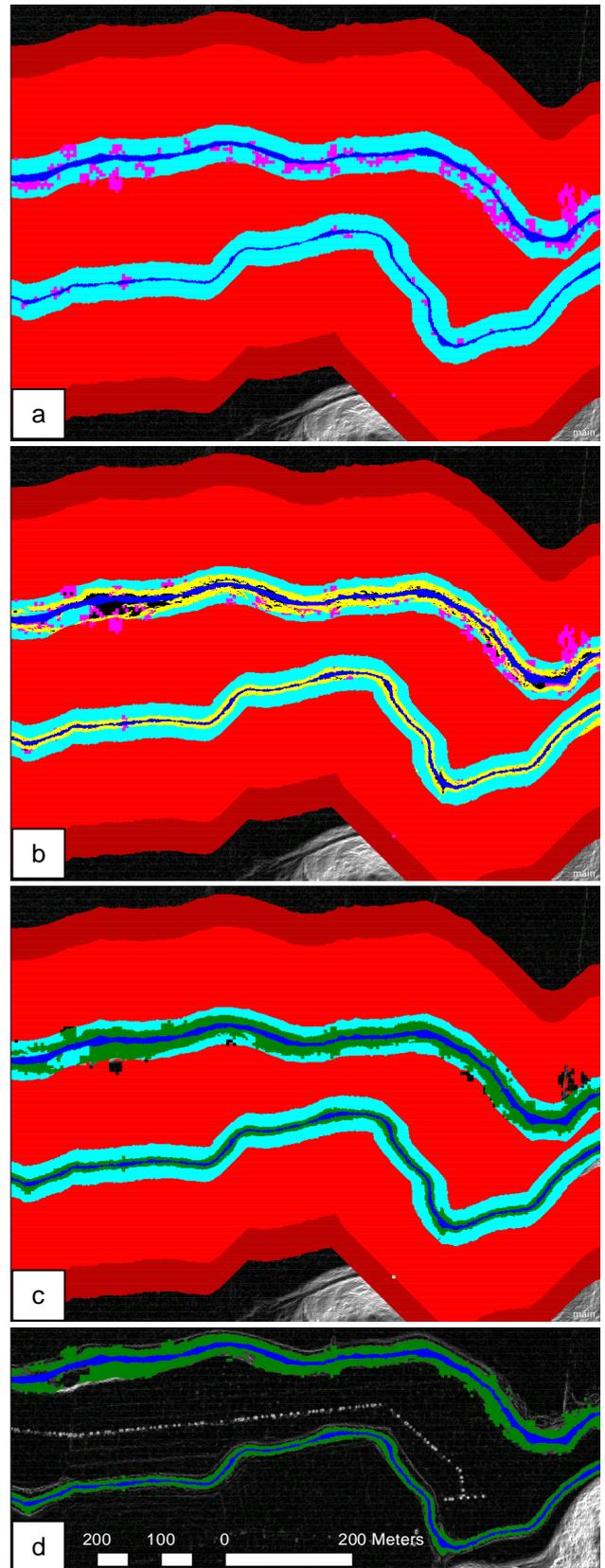


Figure 5. Mapping riparian zones from the LiDAR derived DTM, slope, PPC and streambed layers. The slope layer is used as a backdrop.

Based on field observations, a DTM value of 5 m above the streambed was set as the maximum elevation for riparian zones within a distance of 100 m from the streambed using the relational feature function (Figure 5c). Riparian canopy vegetation extending beyond the edge of the bank top till provides riparian zone functions in terms of habitat and corridor continuity. Therefore, riparian canopy along the external perimeter was included as part of the riparian zone when PCC was > 70%. The shrinking algorithm was used for this process (Figure 5d).

## 2.6 Validation

The field measurements of streambed and riparian zone widths were used for validation of the GEOBIA classification results. The validation was performed using scatter plots and calculating the related coefficient of determination ($R^2$) and root mean square error (RMSE). A total of 35 field measurements of streambed and riparian zone widths were used for the validation.

## 3. RESULTS AND DISCUSSION

Substitution of most of the time and power consuming segmentation and object growing processes with the pixel-based object resizing algorithm using the growing, shrinking and coating modes proved very effective for reducing the processing time. This significant reduction in processing time was possible without affecting the mapping accuracies. Also, tiling of the study area was not necessary anymore compared to the approach of Johansen et al. (2010), which required multiple tiles to be developed and processed individually because of the use of chessboard segmentations producing very large numbers of objects. Reducing the number of tiles or eliminating the need for tiling and stitching processing avoids errors in the classification due to biases along the tiling edges (Tiede and Hoffmann, 2006).

## 3.1 Validation

The comparison of field assessed streambed and riparian zone widths with those derived from the LiDAR data and GEOBIA showed high correlation with no distinct outliers (Figures 6 and 7). Measurements of streambed width were very accurately mapped, which may have been facilitated by the lack of water in most streams at the time of LiDAR data captured. The measurements of wider streambeds were mainly located within a reservoir, where the toes of the banks were poorly defined because of the very limited bank slopes. This added some uncertainly to the GEOBIA identification of the streambed edges. LiDAR data with higher point densities may be more suitable for streams with no distinct bank toes.

Field and LiDAR derived measurements of riparian zone width matched up in most cases, but did generally show larger variation than the streambed width measurements. In general, the use of LiDAR data and the developed GEOBIA approach resulted in an underestimation of riparian zone width based on the best-fit equation presented in Figure 7. In the majority of cases, where riparian zone width was underestimated, the riparian zone had limited canopy cover appearing on relatively flat stream banks, such as the inside sections of meander bends (Figure 8). Because of the reliance on identification of bank slopes and/or canopy cover bordering the mapped streambeds,

the rule set resulted in an underestimation of riparian zone width in some areas. This may be improved in future work through identification of meander bends based on the shape of the streambed and application of specific processes for these areas to facilitate identification of riparian zone extent. This may be done using the DTM to identify the bank top/riparian zone external edge on the outside of meander bends and match this elevation level to the inside of the meander bend to delineate the external riparian zone edge in meander bends with limited bank slope and canopy cover (ISC, 2006).
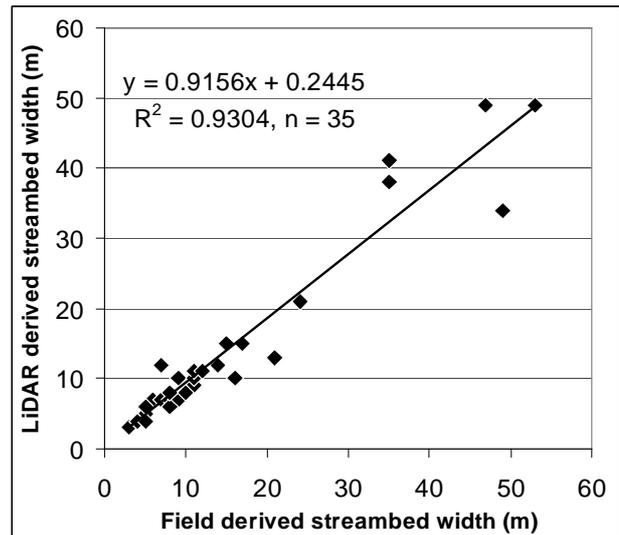


Figure 6. Scatter plot comparing field and LiDAR derived streambed width for 35 field sites. RMSE = 3.6 m.
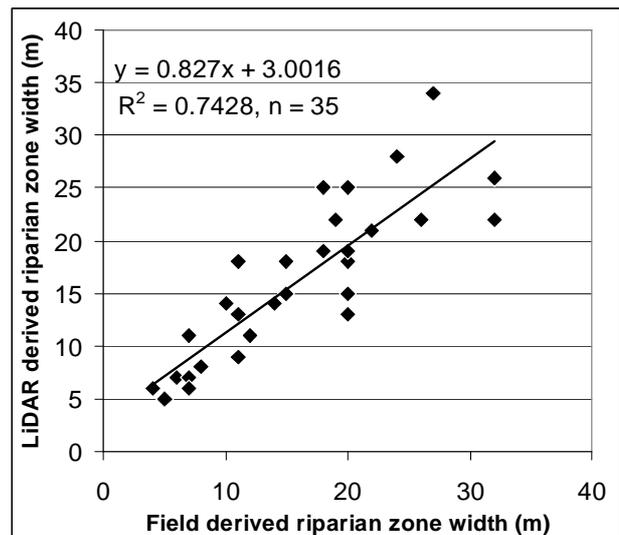


Figure 7. Scatter plot comparing field and LiDAR derived riparian zone width for 35 field sites. RMSE = 3.9 m.

In some situations, the riparian zone width was overestimated if dense non-riparian canopy occurred next to the riparian zone (Figure 8). The rule set may be improved to prevent non-riparian canopy cover from being mapped as part of the riparian zone, if these trees occur at a terrain elevation above the one identified as the bank top. If bank top identification on the one side of the stream with dense non-riparian canopies bordering the riparian zone is not possible, the elevation of the bank top on the opposite side of the stream may be used to

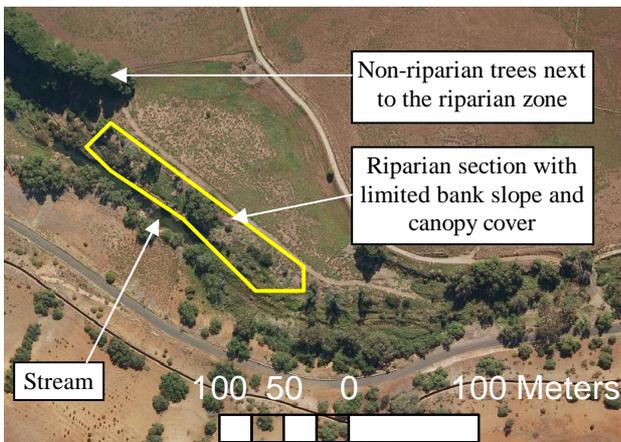determine whether or not to include tree canopies as part of the riparian zone.



Figure 8. Example of riparian zone section (outlined in yellow) with very limited bank slope and canopy cover, which caused underestimation of riparian zone width in some areas. Non-riparian trees next to the riparian zone caused overestimation of riparian zone width. UltracamD image data used for illustration.

## 4. CONCLUSIONS

This research presented a GEOBIA approach for accurate and time-effective mapping of streambed and riparian zone extents based on LiDAR derived DTM, slope and PPC layers as well as an additional rasterised stream centreline shapefile. To improve processing power and time, the rule set relied heavily on the new pixel-based object resizing algorithms in eCognition 8. Through a combination of growing, shrinking and coating functions, the streambed and riparian zone widths were mapped with $R^2$ values of 0.93 and 0.74, respectively in relation to field measurements. The developed rule sets also enabled processing of larger areas than previous research without using tiling and stitching functions. As the study area presented a number of different riparian environments from urban and agricultural sites to natural and hilly areas, the rule set may be applicable to other areas for streambed and riparian extent mapping. However, further research is required to reduce the under- and overestimation of riparian zone width in areas with limited canopy cover and bank slope as well as areas with dense non-riparian canopies bordering the riparian zones.

## 5. REFERENCES

Apan, A.A., Raine, S.R., and Paterson, M.S., 2002. Mapping and analysis of changes in the riparian landscape structure of the Lockyer Valley catchment, Queensland, Australia. *Landscape and Urban Planning*, 59, pp. 43-57.

Armston, J., Denham, R., Danaher, T., Scarth, P., and Moffiet, T., 2009. Prediction and validation of foliage projective cover from Landsat-5 TM and Landsat-7 ETM+ imagery for Queensland, Australia. *Journal of Applied Remote Sensing*, 3, pp. 1-28.

eCognition, 2010. *eCognition Developer 8.0.1 User Guide*, Document version 1.2.1, Definiens AG, Munich, Germany.

Hurtt, G., Xiao, X., Keller, M., Palace, M., Asner, G.P., Braswell, R., et al., 2003. IKONOS imagery for the Large Scale Biosphere-Atmosphere Experiment in Amazonia (LBA). *Remote Sensing of Environment*, 88, 111-127.

ISC, 2006. *Index of Stream Condition Users Manual 3rd Edition*, The State of Victoria Department of Sustainability and Environment, Melbourne, Victoria.

Johansen, K., Phinn, S., Dixon, I., Douglas, M., and Lowry, J., 2007. Comparison of image and rapid field assessments of riparian zone condition in Australian tropical savannas. *Forest Ecology and Management*, 240, pp. 42-60.

Johansen, K., Arroyo, L.A., Armston, J., Phinn, S., and Witte, C., 2010. Mapping riparian condition indicators in a sub-tropical savanna environment from discrete return LiDAR data using object-based image analysis. *Ecological Indicators*, 10(4), pp. 796-807.

Naiman, R.J., and Decamps, H., 1997. The ecology of interfaces: riparian zones. *Annual Reviews in Ecology and Systematics*, 28, pp. 621-658.

Tiede, D. and Hoffmann, C., 2006. Process oriented object-based algorithms for single tree detection using laser scanning data. *EARSeL-Proceedings of the Workshop on 3D Remote Sensing in Forestry*, 14th-15th Feb 2006, Vienna, pp. 151-156.

Werren, G., and Arthington, A., 2002. The assessment of riparian vegetation as an indicator of stream condition, with particular emphasis on the rapid assessment of flow-related impacts. In: A. Shapcott, J. Playford, A.J. Franks (Editors), *Landscape Health of Queensland*, pp. 194-222, The Royal Society of Queensland, St Lucia, Australia.

## ACKNOWLEDGEMENTS